# Measurement and Modeling of End Group Concentration Depth Profiles for $\omega$-Fluorosilane Polystyrene and Its Blends

**Patricia A. V. O'Rourke Muisener, Claire A. Jalbert,[†] Caigen Yuan,[‡] John Baetzold,[§] Ralf Mason, Derek Wong, Young Jun Kim, and Jeffrey T. Koberstein***

*Department of Chemical Engineering and the Polymer Program, Institute of Materials Science, University of Connecticut, Storrs, Connecticut 06269-3136*

**Binnur Gunesin**[⊥]

*Mobil Chemical Company, Edison, New Jersey 08817-3378*

*Received October 25, 2002; Revised Manuscript Received February 10, 2003*

ABSTRACT: Angle-dependent X-ray photoelectron spectroscopy (ADXPS) is used to measure end group concentration depth profiles for blends of surface active $\omega$-fluorosilane polystyrene with nonfunctional polystyrene. The fluorine signal is in all cases enhanced at the surface, indicating surface segregation of the lower surface tension fluorosilane end groups. End group segregation is enhanced by an increase in the concentration of $\omega$-fluorosilane polystyrene, an increase in the nonfunctional polystyrene molecular weight, or a decrease in the molecular weight of the $\omega$-fluorosilane polystyrene. A self-consistent mean-field lattice theory is developed to model the surface structure and properties of blends containing end-functional polymers. Lattice model calculations provide estimates of concentration depth profiles as a function of the blend composition, the normalized chain lengths of the blend constituents, and the surface and bulk interaction parameters, $\chi_s$ and $\chi_b$, respectively. Two end-functional polystyrene architectures are considered: $\alpha$-functional polystyrene for which the lattice reference volume is set equal to that of the entire fluorosilane end group and $\alpha,\beta$-functional polystyrene where the fluorosilane end group is assumed to occupy two adjacent lattice sites at the chain end. The lattice model for both architectures provides excellent representations of experimental ADXPS data over a wide range of blend compositions and constituent molecular weights. The $\alpha,\beta$-functional polymer model is shown to be superior on two accounts: the lattice reference volume and polymer repeat unit volumes are similar, and the optimal values of $\chi_s = -2.18$ and $\chi_b = 1.59$, obtained by regression of this model to ADXPS data, are consistent with group contribution estimates of these parameters.

## Introduction

The importance of surface properties in many essential polymer technologies has provided substantial motivation to develop methods for polymer surface modification. The myriad of chemical and physical methodologies that have been reported[1] all share the common goal of controlling the number and type of chemical constituents at the surface. Because the nature of surface modification strategies involves either blending with another polymer or chemical modification of the parent polymer, surface-modified polymers are compositionally and spatially heterogeneous materials. One of the key features of heterogeneous polymer systems, and a critical aspect of many surface modification approaches, is the phenomenon of surface segregation. Molecular fragments, functional groups, or polymer chains of lowest surface energy preferentially segregate to the surface in order to decrease the surface free energy and minimize the overall free energy of the system. Surface segregation is controlled by a balance between the free energy gain associated with the surface tension reduction accompanying surface adsorption and the free energy cost of demixing surface active species from the bulk. Surface segregation phenomenon have been well studied experimentally and theoretically for a wide variety of chemically heterogeneous polymer systems.[2−6]

End-functional polymers[7,8] are a particularly interesting class of chemically heterogeneous materials. They not only serve as convenient model systems that reflect the general behavior of all functional polymers but also constitute a practical means for modifying surface properties without affecting substantial changes in the bulk properties. End-functional polymers are interesting in a conceptual sense because entropic and enthalpic effects are coupled due to chain connectivity. Surface segregation has been studied for end-functional polystyrene[6,9−14] and poly(dimethylsiloxane)[18] using an assortment of experimental techniques. These works demonstrate surface enrichment for end groups of lower surface tension than the chain backbone and surface depletion for end groups of higher surface tension than the chain backbone.

Lattice theories[15−19] provide excellent predictions of surface tensions for block and random copolymers of ethylene oxide and propylene oxide[15] as well as for $\alpha,\omega$-functional poly(dimethylsiloxane).[18] Most recently, we

[†] Current address: IMAK, 310 Commerce Drive, Amherst, NY 14228-2396.

[‡] Current address: Institute of Petrochemical Engineering, East China University of Science and Technology, Jin-Shan Wei, Shanghai, China 200450.

[§] Current address: 3M Display Technology Center, St. Paul, MN 55144-1000.

[⊥] Current address: Dutoit/Gunesin CS, Rue Ami-Levrier 11, CH-1201, Geneva, Switzerland.

* To whom correspondence should be addressed. Current address: Columbia University, MC4721, Department of Chemical Engineering, 500 West 120th Street, New York, NY 10027. E-mail: jk1191@columbia.edu; Tel 212-854-3120; FAX 212-854-3054.

10.1021/ma021623v CCC: $25.00 
Published on Web 03/26/2003

**Table 1. Characteristics of Nonfunctional and *ω*-Fluorosilane Polystyrenes**

| *ω*-fluorosilane polystyrenes | | | | nonfunctional polystyrenes | |
|---|---|---|---|---|---|
| polymer | $M_w$ | $M_w/M_n$ | functionality (*f*) | polymer | $M_w$ |
| PSF5 | 5 300 | 1.04 | 0.89 | PS4 | 4 000 |
| PSF5.4 | 5 400 | 1.09 | 0.67 | PS9 | 9 000 |
| PSF10 | 10 900 | 1.06 | 0.78 | PS19 | 19 000 |
| PSF17 | 17 300 | 1.16 | | PS35 | 34 500 |
| PSF25 | 25 000 | 1.12 | 0.85 | PS63 | 63 000 |
| PSF35 | 35 500 | 1.05 | | PS127 | 127 000 |
| PSF148 | 148 000 | 1.06 | 1.00 | PS350 | 350 000 |
| | | | | PS1100 | 1 100 000 |

have employed the lattice model to investigate optimal chain architectures for the molecular design of functional polymer surfaces.[19] Angle-dependent X-ray photoelectron spectroscopy (ADXPS) has been applied to characterize composition−depth profiles for α,*ω*-aminoalkyl poly(dimethylsiloxane)[20] and *ω*-fluorosilane polystyrene;[7,21] however, theoretical predictions of functional group concentration depth profiles for end-functional polymers remain to be tested.

In this paper, we report ADXPS measurements of end group concentration depth profiles for *ω*-fluorosilane polystyrene and its blends with nonfunctional polystyrene and compare these results to an extension of the lattice theory for functional polymer blends developed herein. We also compare lattice model predictions to previously reported[21] end group concentration depth profiles for *ω*-fluorosilane polystyrenes.

## Experimental Section

**Materials.** *ω*-Functional polystyrenes terminated with a fluorosilane end group were synthesized by anionic polymerization of styrene in cyclohexane at 60 °C using *sec*-butyllithium as initiator. Styrene monomer was distilled over calcium hydride, and cyclohexane solvent was distilled over sulfuric acid. The reaction was terminated with tridecafluoro-1,1,2,2-tetrahydrooctyl-1-dimethylchlorosilane (Huls-America) to provide an end group of structure [$-Si(CH_3)_2-(CH)_2(CF_2)_5-CF_3$]. Nonfunctional polystyrenes were purchased from Polysciences.

**Sample Characterization.** Gel permeation chromatography (GPC) was used to determine the molecular weights and molecular weight distributions of polymer samples referenced to polystyrene standards. The system used was a Waters 150-C consisting of a model 510 pump, model 410 refractometer, model 840 data station, and four Ultrastyragel columns with pore sizes of 1000, 100, 50, and 10 nm. Tetrahydrofuran was the mobile phase, and the system was operated at room temperature. Elemental analysis (Galbraith Laboratories) was used to determine the fluorine content of *ω*-fluorosilane polystyrenes. The efficiency of end functionalization or functionality, *f*, is defined as the ratio of fluorine content obtained from elemental analysis to the fluorine content expected from the chemical formula and the measured molecular weight. Characterization results for the polymers used are summarized Table 1. In the nomenclature adopted, PSF is *ω*-fluorosilane polystyrene, PS is nonfunctional polystyrene, and the number that follows denotes the nominal molecular weight in thousands. The designation PSF10, for example, refers to 10 kDa *ω*-fluorosilane polystyrene.

A Perkin-Elmer DSC 7 was used to determine whether the functional end groups formed any crystalline or liquid crystalline aggregates. The cell was purged with dry nitrogen, and the temperature was scanned from 30 to 350 °C at 10 °C/min. No thermal transitions were detected that might be associated with phase transitions of the fluorosilane end groups.

Angle-dependent X-ray photoelectron spectroscopy measurements were made with a PHI system 5300 spectrometer equipped with a monochromatic Al Kα source providing 1487 eV X-rays with a line width of 0.85 eV. To assess the chemical stability of the fluorinated end groups, sample PSF10 was exposed to the X-ray beam for 24 h, and the fluorine-to-carbon ratio was measured as a function of time. The fluorine signal decreased with exposure time and, after 6 h of exposure to the X-rays, was reduced by about 10% due to photoelectron damage.[21] To minimize the fluorine loss, samples were exposed to the X-ray beam for 4 h or less. Data for different takeoff angles were collected in random order in order to block systematic errors. Data for several takeoff angles were repeated whenever a new sample was introduced in order to ensure reproducibility of the data. A typical ADXPS data set as reported in this paper is thus a collection of data from 5−6 samples superimposed onto one graph. Although it is difficult to establish absolute errors for XPS data, the limited scatter of data observed in the superimposed composite graphs illustrates that the repeatability of the data is excellent, generally falling within a range defined by 2−3 times the diameter of the symbols shown in the graphs of ADXPS data.

**Sample Preparation.** Neat films of *ω*-fluorosilane polystyrene were prepared by spin-coating solutions of the polymer onto silicon wafers. Polymers were dissolved in chloroform and filtered through a 0.2 mm Teflon filter prior to spin-coating. The substrates, 3 in. silicon (111) wafers (Motorola, Inc.), were rinsed three times with filtered chloroform before use. The concentration of the polymer solution was 15% (w/v). Spin-coated films were annealed in a vacuum for 16 h at 165 °C to attain equilibrium. The annealed samples were cooled to room temperature in a vacuum and introduced to the X-ray photoelectron spectrometer chamber within 6 h of being removed from the vacuum chamber. While direct measurements were not made, these conditions are expected to produce polymer surfaces with minimal surface roughness. Blends of *ω*-fluorosilane polystyrene and nonfunctional polystyrene were prepared by codissolution in cyclohexane. The surface segregation of fluorocarbon chain ends in blends generally reached apparent equilibrium after annealing for 5 min at 165 °C. Most blends were therefore equilibrated by annealing for 30 min at 165 °C.

## Lattice Model Calculations

The characterization results for *ω*-fluorosilane polystyrenes in Table 1 show that the end group functionalization/termination reaction does not go to completion. If it is assumed that polymers that are not terminated with the fluorosilane end group are terminated with a proton, then the neat end-functional polymers are actually blends of end-functional and nonfunctional polymers. Similar reasoning leads to the conclusion that binary blends of end-functional polystyrene with nonfunctional polystyrene must be treated as a ternary blend of one end-functional polymer and two different nonfunctional polymers.

Lattice theories have been developed for nonfunctional polymer blends,[22,23] but not for blends including a functional polymer. Self-consistent mean-field theories[24,12] have been applied previously to analyze surface adsorption isotherms in end-functional polymer blends. Unfortunately, these theories do not provide end group concentration depth profiles. We have therefore extended the lattice theory herein in order to model the surface properties of binary and ternary blends containing one end-functional polymer. The basis of the model is a cubic lattice confined between two impenetrable surfaces that are well enough separated to form a bulklike region in the center of the film. Properties are symmetric about the center of the film since the two walls are defined to be identical. The number of total chain segments, or normalized chain length, *r*, for each polymer in the blend is defined as the total volume of the chain divided by the reference volume of a lattice

site

$$r = \frac{Zv_r + v_e}{v_{ref}} \quad (1)$$

$Z = (M - m_e)/v_r$ is the number of polymer repeat units of volume $v_r$, $v_e$ and $m_e$ are the end group volume and mass, respectively, $v_{ref}$ is the reference volume for a single lattice site, and $M$ is the molecular weight of the entire polymer chain including the end group. If the functionality of the "neat" end-functional polymer is less than unity (Table 1), it must be considered as a mixture of end-functional polymer and proton-terminated nonfunctional polymer. In this case, the normalized chain length for the nonfunctional component is calculated by (1) with $v_e = 0$. Binary blends of functional polymers with incomplete functionalization and nonfunctional polymers must therefore be considered as ternary blend systems that are characterized by three chain lengths: two chain lengths appropriate for the functional polymer itself and a third chain length for the added nonfunctional polymer (Table 1).

Two different chain structures are considered in the calculations based upon the use of two different reference volumes. If the reference volume required in (1) is set equal to the volume of the entire fluorosilane end group, $-Si(CH_3)_2-(CH)_2(CF_2)_5CF_3$, the polymer is considered as α-fluorosilane polystyrene with chain length $r_\alpha$ (note that $\omega$-functional chains are equivalent to α-functional chains in the lattice model). In this case, the molecular weight of the end group is 405 g/mol, and the reference volume is set to the volume of the end group, 253.5 $cm^3$/mol, calculated by group contribution methods.[25] One drawback of using the entire fluorinated end group as the reference volume is that the volume and molecular weight of the end group are much larger than those of the polystyrene repeat unit. This drawback is alleviated by use of a normalized chain length $r_{\alpha,\beta}$, which assumes the chain has α,β-functional architecture with two adjacent functional groups on the end of the chain. In this case, the reference volume required in (1) is taken as one-half of the volume of the fluorosilane end group, 126.75 $cm^3$/mol, a value that is closer to the volume of the polystyrene repeat unit,[25] 98.0 $cm^3$/mol. The reference volume selected also determines the appropriate chain length to be used to model the nonfunctional polystyrenes according to (1).

The surface interaction parameter describes the preference of the functional end group for the surface compared to that of the chain backbone and is defined by

$$\chi_s = \frac{U_s^e - U_s^r}{k_B T} = \frac{(\gamma_e - \gamma_r)a}{k_B T} \quad (2)$$

where the subscripts e and r indicate properties associated with the end groups and repeat units, respectively. $U_s$ is the energy of surface adsorption of each constituent with surface tension $\gamma$, $k_B$ is the Boltzmann constant, $T$ is the temperature, and $a = v_{ref}^{2/3}$ is the surface area of a lattice site. The surface interaction parameter is negative for $\omega$-fluorosilane polystyrene because the end groups are of lower surface tension and therefore absorb preferentially at the surface.

Quantitative predictions of end group concentration depth profiles for $\omega$-fluorosilane polystyrenes must also consider the effects of bulk interactions between the end group and its polystyrene backbone because of the large magnitude of the bulk interaction parameter. The bulk interaction parameter can be calculated from regular solution theory, which should be applicable in the present case where only dispersive interactions are expected between the polystyrene backbone and the fluorosilane end group. The bulk interaction parameter can be estimated from solubility parameters according to

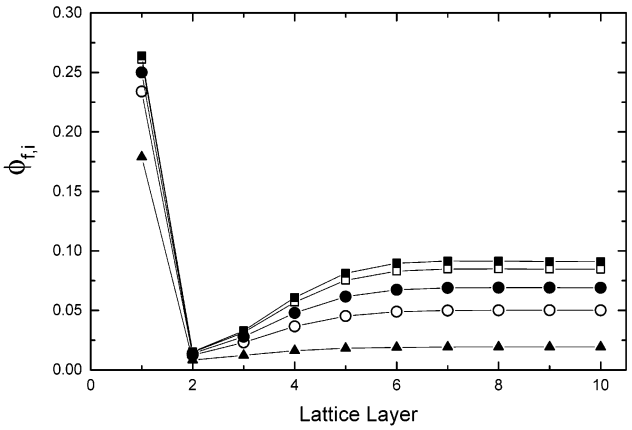


**Figure 1.** End group concentration depth profiles for blends of α-functional polymer ($r_\alpha = 11$, $\chi_s = -3$, $\chi_b = 1.85$) with nonfunctional polymer ($r_n = 11$). The fraction of end-functional polymer in the blends is 100% (filled squares), 90% (open squares), 70% (filled circles), 50% (open circles), and 20% (filled triangles).

$$\chi_b = v_{ref}^{1/3} \frac{(\delta_e - \delta_r)^2}{RT} \quad (3)$$

$R$ is the gas constant, $\delta_e$ is the solubility parameter of the end group, and $\delta_r$ is the solubility parameter of the repeat unit. A zero-order continuation scheme is implemented to account for the bulk interactions when solving for the free segment probabilities in the lattice calculations. Calculations for a given chain length and $\chi_s$ value start with the bulk interaction parameter set to zero and then proceed to progressively increasing values of $\chi$ using the last solution as an initial guess for the next one. A step size of $\Delta\chi = 0.1$ proved to be adequate for this purpose.

The parameters required in the lattice calculation are the chain length of the end-functional polymer, the chain length of the nonfunctional polymer(s) in the blend, the functionality of the end-functional polymer, the fraction of end-functional polymer in the blend, the surface interaction parameter, $\chi_s$, and the bulk interaction parameter, $\chi_b$.

The lattice calculations provide a prediction of the concentration depth profiles for the end group and repeat units of each polymer in the blend. Because the end-functional and nonfunctional polymers have the same polystyrene repeat unit, the repeat unit volume fractions are added together to reduce the solution to concentration profiles for two constituents: the end group and the repeat unit.

Typical end group concentration depth profiles predicted by the lattice theory are shown in Figure 1. The volume fraction of functional groups in lattice layer $i$ is denoted $\phi_{f,i}$. The basic characteristics of the end group distributions are similar to those of neat end-functional polymers.[15−19] Surface enrichment of the low-energy end

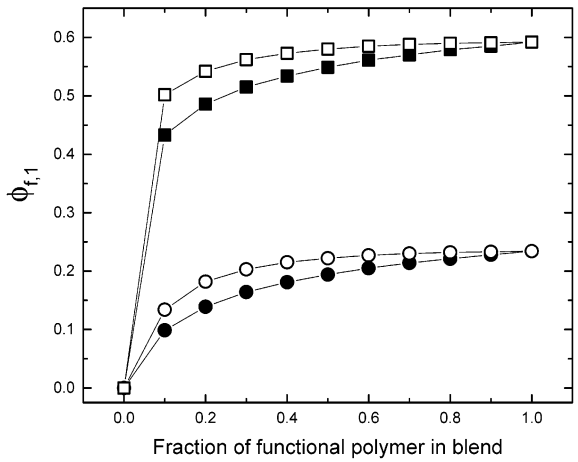


**Figure 2.** Surface functional group concentration vs bulk composition for functional polymer blends: (a) α-functional polymer ($r_\alpha = 11$, $\chi_s = -3$, $\chi_b = 1.85$) blended with nonfunctional polymer (open circles, $r_n = 11$; filled circles, $r_n = 201$) and (b) α,*β*-functional polymer ($r_{\alpha,\beta} = 11$, $\chi_s = -3$, $\chi_b = 1.85$) blended with nonfunctional polymer (open squares, $r_n = 11$; filled squares, $r_n = 201$).

groups is confined to the first lattice layer, while deeper layers exhibit a depletion gradient with gradually rising concentration over a depth comparable to the chain dimensions. The interesting surface structure arises from the coupling of entropic and enthalpic effects when two chemically heterogeneous moieties are placed on the same chain and is discussed in detail in previous publications.[17,18]

The degree of surface enrichment attained is determined by a balance between three factors: the surface free energy reduction that occurs when low-energy end groups adsorb in the first lattice layer, the configurational entropy loss due to deformation of the α-functional polymer when the end groups adsorb, and the exchange chemical potential associated with moving α-functional polymers from the bulk to the surface. The surface concentration of low-energy end groups increases with content of the α-functional polymer in the blend, and there is a commensurate increase in the magnitude of the depletion gradient due to connectivity between the end group and chain backbone. The depth of depletion gradients depends on both the chain length of the α-functional polymer and its bulk composition in the blend.

In a previous paper,[19] the optimum architecture for promoting surface segregation in a polymer with two low surface energy functional groups was shown to be an α,*β*-functional polymer with two attractive functional groups adjacent to one another at the polymer chain end. The surface properties of α,*β*-functional polymers (squares) are directly compared to those of α-functional polymers (circles) in Figure 2. For both matrix molecular weights, the α,*β*-functional polymers exhibit enhanced enrichment of functional groups at the surface compared to the α-functional polymers. The surface concentration of functional groups begins to reach a plateau for the larger matrix molecular weight, $r = 201$, when the blend contains 50% α,*β*-functional polymer.

**Angle-Dependent X-ray Photoelectron Spectroscopy Analysis.** The basis of angle-dependent X-ray photoelectron spectroscopy (ADXPS) is ejection of a core level electron by an incident X-ray photon. The kinetic energy of ejected photoelectrons, $E_{i,k}$, is specific to the atom, *i*, and orbital, *k*, from which the photoelectron originated and is given by

$$E_{i,k} = h\nu - \mathrm{BE} - \mathrm{WF} \tag{4}$$

BE is the binding energy of the electron (specific to the atom and orbital), $h\nu$ is the energy of the incident X-rays, and WF is the instrument work function.

Some of the ejected photoelectrons suffer inelastic collisions as they travel through the sample, whereupon they lose their original kinetic energy and the related compositional information that they carry. The probability of photoelectron escape without inelastic collision is $e^{-z/\lambda \sin\theta}$, where *z* is the depth, $\lambda$ is the electron mean free path, and $\theta$ is the photoelectron takeoff angle between the detector and the plane of the surface. An escape depth from which 95% of the photoelectrons emanate can therefore be defined as $d = 3\lambda \sin\theta$. Depth profiling is accomplished by varying the takeoff angle, with lower takeoff angles corresponding to shallower depths.

The resultant ADXPS integral depth profile is of the form[26]

$$N_{i,k}(\theta) = K_{i,k}\int_0^z n_i(z) \exp(-z/\lambda_{i,k} \sin\theta)\, dz \tag{5}$$

$N_{i,k}(\theta)$ is the peak signal intensity of generated photoelectrons for the *k*th shell of atom *i* at a takeoff angle $\theta$, $\lambda_{i,k}$ is the mean free path, $n_i(z)$ is the atomic concentration (atoms/cm$^3$) as a function of depth *z*, and $K_{i,k}$ is a sensitivity factor. The end group and repeat unit concentration profiles predicted by the lattice model must be converted into atomic concentration depth profiles, $n_i(z)$, and integrated according to (5) in order to make comparisons between theoretical predictions and experimental ADXPS data.

There are several expressions available in the literature for calculating photoelectron mean free paths. For example, Ashley[27] showed that for many organic polymers

$$\lambda_{i,k} = \frac{M}{\rho n} E_{i,k}/(13.6 \ln E_{i,k} - 17.6 - 1400/E_{i,k}) \tag{6}$$

*M* is the molecular weight of the repeat unit (g/mol), *n* is the number of valence electrons in the repeat unit, and $\rho$ is the density (g/cm$^3$).

To evaluate the integral in (5), the polymer surface region is divided into a number of discrete layers of equal thickness, *t*, as in the lattice model. The layers are counted from the surface ($L = 1$) to some arbitrary layer within the bulk ($L = n$). Because the composition−depth profiles provided by the lattice model are discretized with a depth increment given by the lattice dimension, it is convenient to set the layer thickness equal to the lattice dimension in the lattice model, that is, $t = \nu_{ref}^{1/3}$.

To compare the results of lattice theory to experimental ADXPS data, the concentration of element *i* within a layer *L*, $n_i(L)$, is calculated by the lattice theory. Starting with the first layer, (5) is applied, integrating from the surface ($z = 0$) to the bottom of the first layer ($z = t$), to yield an expression for the signal intensity, $N_{i,k}(1)$, emanating from the first layer:

$$N_{i,k}(1) = K_{i,k}\lambda_{i,k} n_i(1) \sin\theta\left[1 - \exp\left(\frac{-t}{\lambda_{i,k} \sin\theta}\right)\right] \tag{7}$$

For the second layer, the attenuation due to inelastic scattering in the overlayer must be taken into account, yielding

$$N_{i,k}(2) = K_{i,k}\lambda_{i,k}n_i(2)\sin\theta\left[1 - \exp\left(\frac{-t}{\lambda_{i,k}\sin\theta}\right)\right] \exp\left(\frac{-t}{\lambda_{i,k}\sin\theta}\right) \quad (8)$$

A general expression for the signal intensity emanating from any layer, $L$, can therefore be written as

$$N_{i,k}(L) = K_{i,k}\lambda_{i,k}n_i(L)\sin\theta\left[1 - \exp\left(\frac{-t}{\lambda_{i,k}\sin\theta}\right)\right] \exp\left(\frac{t(1-L)}{\lambda_{i,k}\sin\theta}\right) \quad (9)$$

By taking the sum of the intensities of all layers, the total signal intensity from element $i$ at a particular takeoff angle, $\theta$, is obtained:

$$N_{i,k}(\theta) = K_{i,k}\lambda_{i,k}\sum_{L=1}^{L=n} n_i(L)\sin\theta\left[1 - \exp\left(\frac{-t}{\lambda_{i,k}\sin\theta}\right)\right] \exp\left(\frac{t(1-L)}{\lambda_{i,k}\sin\theta}\right) \quad (10)$$

In presenting and analyzing ADXPS data, it is common to report the ratio of signals for two elements because this representation eliminates a number of uncertainties such as variations in X-ray flux. In the case of end-functional polymers, the ratio of a signal associated with an atom in the end group to one associated with an atom in the chain backbone is usually reported. Extension of the treatment presented above yields the following expression for the ratio of signals from atoms 1 and 2:

$$\frac{N_1(\theta)S_2}{N_2(\theta)S_1} = \frac{\sum_{L=1}^{L=n} n_1(L)\sin\theta\left[1 - \exp\left(\frac{-t}{\lambda_1\sin\theta}\right)\right]\exp\left(\frac{t(1-L)}{\lambda_1\sin\theta}\right)}{\sum_{L=1}^{L=n} n_2(L)\sin\theta\left[1 - \exp\left(\frac{-t}{\lambda_2\sin\theta}\right)\right]\exp\left(\frac{t(1-L)}{\lambda_2\sin\theta}\right)} \quad (11)$$

$S$ is an overall sensitivity factor for each element and is equal to $K\lambda$. Most XPS instruments are programmed with overall sensitivity factors for the electron orbitals of a variety of atoms, either supplied by the manufacturer or determined through calibration with standards of known atomic composition. In this case, the experimental data are already corrected for sensitivity factors, and it is not necessary to calculate the sensitivity factors in order to compare theoretical predictions with XPS experiments.

Inputs that are required to calculate the signal intensity ratio for two elements include the lattice layer thickness and composition in each lattice layer (supplied by the lattice theory calculations), the takeoff angle used in the experiment, and the mean free paths for both components calculated from (6). In this paper we calculate the ratio of signal intensities of fluorine, which originates from the end group, to carbon, which is present in both the chain backbone and the end group.

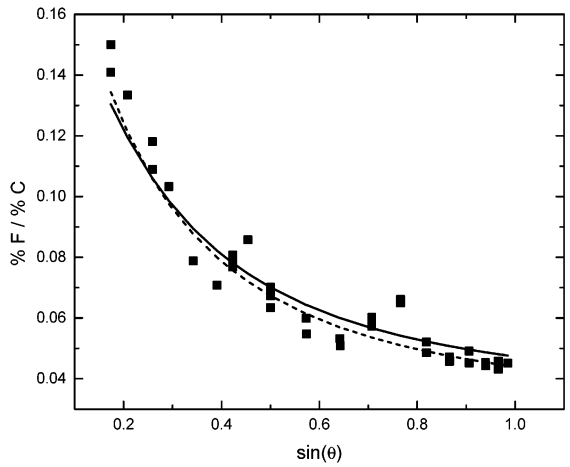


**Figure 3.** Fluorine-to-carbon atomic ratios for PSF5 as a function of the sine of the takeoff angle. The solid line is the profile predicted for a blend of 89% α-functional polymer ($r_\alpha$ = 19, $\chi_s$ = −3.34, $\chi_b$ = 4.7) with 11% nonfunctional polymer ($r_n$ = 18). The dashed line is the profile predicted for a blend of 89% α,β-functional polymer ($r_{\alpha,\beta}$ = 39, $\chi_s$ = −2.18, $\chi_b$ = 1.59) with 11% nonfunctional polymer ($r_n$ = 38).

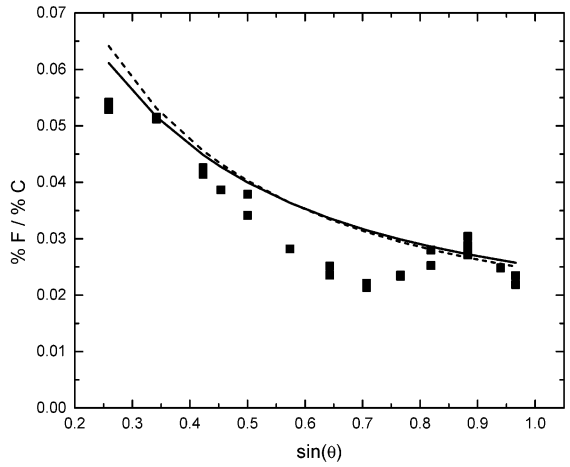


**Figure 4.** Fluorine-to-carbon atomic ratios for PSF10 as a function of the sine of the takeoff angle. The solid line is the profile predicted for a blend of 78% α-functional polymer ($r_\alpha$ = 40, $\chi_s$ = −3.34, $\chi_b$ = 4.7) with 22% nonfunctional polymer ($r_n$ = 39). The dashed line is the profile predicted for a blend of 78% α,β-functional polymer ($r_{\alpha,\beta}$ = 81, $\chi_s$ = −2.18, $\chi_b$ = 1.59) with 22% nonfunctional polymer ($r_n$ = 79).

## Results and Discussion

The fluorine-to-carbon atomic ratios for "neat" ω-fluorosilane polystyrenes as a function of the takeoff angle are shown in Figures 3−6 for four different molecular weights. For all polymers, the surface is enriched in fluorine, indicating preferential surface adsorption of the fluorosilane end groups. The degree of enrichment decays as the probe depth increases (i.e., with increasing $\sin\theta$). An interesting feature that can be seen in these data is the presence of apparent local maxima and minima in the integral depth profiles. This is especially apparent in the data for PSF5 (Figure 3). The depths at which the local maxima appear are dependent on molecular weight and scale roughly with the radii of gyration of the polymers. After significant effort, we have been unable to find a model that can reproduce

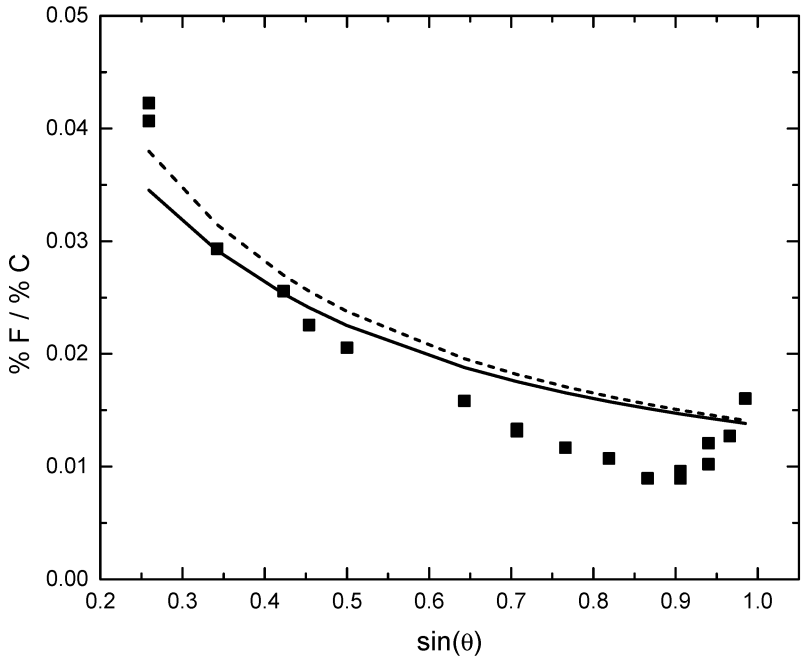


**Figure 5.** Fluorine-to-carbon atomic ratios for PSF25 as a function of the sine of the takeoff angle. The solid line is the profile predicted for a blend of 85% α-functional polymer ($r_\alpha = 93$, $\chi_s = -3.34$, $\chi_b = 4.7$) with 15% nonfunctional polymer ($r_n = 92$). The dashed line is the profile predicted for a blend of 85% α,*β*-functional polymer ($r_{\alpha,\beta} = 187$, $\chi_s = -2.18$, $\chi_b = 1.59$) with 15% nonfunctional polymer ($r_n = 186$).

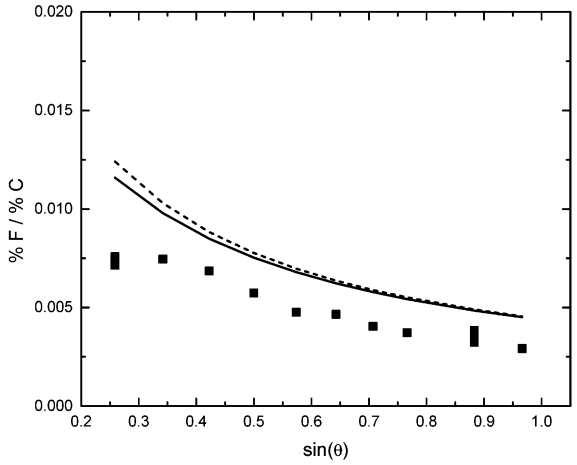


**Figure 6.** Fluorine-to-carbon atomic ratio for PSF148 as a function of the sine of the takeoff angle. The solid line is the profile predicted for 100% α-functional polymer ($r_\alpha = 554$, $\chi_s = -3.34$, $\chi_b = 4.7$). The dashed line is the profile predicted for 100% α,*β*-functional polymer ($r_{\alpha,\beta} = 1112$, $\chi_s = -2.18$, $\chi_b = 1.59$).

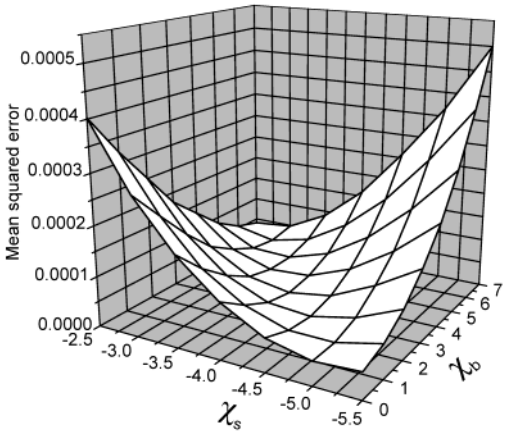


**Figure 7.** Sum of mean-squared errors between predicted and observed depth profiles for PSF5, PSF10, and PSF25 as a function of $\chi_s$ and $\chi_b$. The model predictions used to determine the mean-squared errors were based upon an α-functional architecture for PSF.

this feature of the concentration depth profiles and can provide no conclusive explanation of its origins at the present time.

The solid lines in Figures 3−6 represent the surface composition−depth profiles predicted from the lattice model assuming that PSF is an α-functional polymer. The parameters required for the lattice calculations: the chain lengths for the end-functional polymer and the nonfunctional polymer in the blend, the functionality of the end-functional polymer, and the fraction of end-functional polymer in the blend are taken from Table 1.

To obtain the theoretical profiles, the surface and bulk interaction parameters were taken as adjustable parameters with their optimal values determined by regression of lattice model calculations to the entire set of ADXPS data for all samples. The theoretical atomic concentration ratios as a function of sin($\theta$) were calculated for a set of $\chi_s$ and $\chi_b$ values within the ranges $-1 < \chi_s < -5$ and $1 < \chi_b < 7$. The theoretical integral depth profiles were then directly compared to the experimentally obtained profiles, and the mean-squared error for each parametric set was calculated and summed over all of the data sets to obtain an overall error minimization. The total mean-squared error, summed for regressions to all of the data for PSF5, PSF10, and PSF25, is presented in Figure 7 as a function of $\chi_s$ and $\chi_b$. The data do not show a global minimum, but rather a trough of roughly equivalent minimal mean-squared errors. Many pairs of $\chi_s$ and $\chi_b$ values therefore provide reasonable representations of the data, samplings of which are listed in Table 2 along with the corresponding mean-squared errors.

Because it is somewhat awkward to discuss the results in terms of volume-dependent interaction pa-

**Table 2. Optimal Pairs of $\chi_s$ and $\chi_b$ Values That Can Reproduce ADXPS Data Assuming an α-Functional Polymer Architecture and the Corresponding Mean-Squared Error Summed over All Data Sets[a]**

| $\chi_s$ | $\chi_b$ | total mean-squared error | $\gamma_e$ from eq 2 | $\delta_e$ from eq 3 |
|---|---|---|---|---|
| −2.5 | 7 | $4.05 \times 10^{-5}$ | 21.67 | 5.06 |
| −3 | 6 | $3.89 \times 10^{-5}$ | 18.01 | 5.36 |
| −3.5 | 4 | $4.21 \times 10^{-5}$ | 14.35 | 6.042 |
| −4 | 3 | $3.94 \times 10^{-5}$ | 10.68 | 6.45 |
| −4.5 | 2 | $4.18 \times 10^{-5}$ | 7.02 | 6.94 |
| −5 | 1 | $4.58 \times 10^{-5}$ | 3.35 | 7.57 |
| −5.5 | 0 | $5.11 \times 10^{-5}$ | −0.31 | 9.1 |

[a] The values of the end group surface tension, $\gamma_e$, and solubility parameter, $\delta_e$, are calculated from eqs 2 and 3.

rameters, a change of variables was affected so that regression results were cast in terms of two more familiar volume-independent parameters: the surface tension and solubility parameter of the functional end group. The change of variables is accomplished by applying the definitions of $\chi_s$ and $\chi_b$ represented by (2) and (3) with the known surface tension[1] and solubility parameter[28] of polystyrene (40 dyn/cm and 9.1 $cal^{1/2}$ $cm^3$, respectively). Table 2 shows the range of subsequent calculated pairs of end group solubility parameter and surface tension values that are capable of reproducing the experimental ADXPS profiles. The global optimum parameter set of $\chi_s$ and $\chi_b$ can then be established by determining which set of end group solubility parameter and surface tension values is self-consistent or compares best to literature values of compounds with similar structure as that of the end group.

On the basis of the similarity of their structures, the solubility parameter and surface tension of the end group might be expected to be similar to those for poly(tetrafluoroethylene)[1,25] (PTFE), 6.2 $cal/cm^{3/2}$ and 21.5 dyn/cm, respectively. These values, however, are not consistent with the parameter pairs in Table 2 that were determined assuming α-functional architecture for the *ω*-fluorosilane polystyrene polymers.

A global optimum can also be established by recognizing that a relationship between $\chi_s$ and $\chi_b$ can be established by group contribution methods. Group contribution methods (see Appendix) provide relationships between the solubility parameter of the end group and its surface tension. Since $\chi_s$ and $\chi_b$ are functions of these same two variables according to (2) and (3), a group contribution relationship between $\chi_s$ and $\chi_b$ can be established. The optimal pair of $\chi_s$ and $\chi_b$ values that fit the ADXPS data can then be determined by the intersection of the experimental relationship between $\chi_s$ and $\chi_b$ obtained from the fit of ADXPS data (Table 2) with the group contribution relationship between $\chi_s$ and $\chi_b$.

Figure 8 compares $\chi_s$ vs $\chi_b$ obtained by the Hildebrand and Scott group contribution relationship[29] with experimental results obtained by modeling PSF as an α-functional polymer. The intersection of the two relationships occurs at $\chi_s = -3.34$ and $\chi_b = 4.7$. When the Koenhen and Smolder group contribution relationship[30] is used, the intersection occurs at $\chi_s = -3.34$ and $\chi_b = 4.58$. The solid lines in Figures 3−6 were calculated using $\chi_s = -3.34$ and $\chi_b = 4.7$. While these values appear to give reasonable representations of the data, they are not consistent with the values $\chi_s = -2.7$ and $\chi_b = 2.54$ calculated by (2) and (3) using the group contribution estimates of $\gamma_e$ and $\delta_e$ presented in Table 3. We therefore

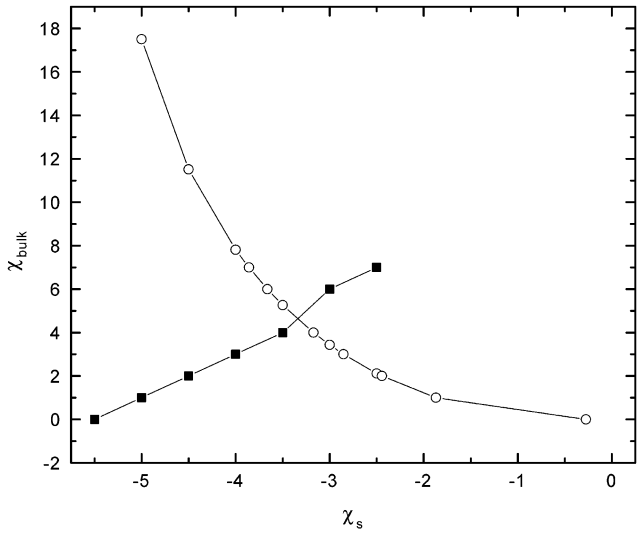


**Figure 8.** Relationship between $\chi_s$ and $\chi_b$: predicted by the Hildebrand and Scott formulas (circles) and obtained from optimal comparisons to the data when PSF is modeled as an α-functional polymer (squares).

conclude that modeling the *ω*-fluorosilane polystyrene as an α-functional polymer does not adequately characterize the system.

A possible explanation for failure of the α-functional polymer model is its use of the volume of the end group as the reference volume. The end group volume, 253.5 $cm^3$/mol, is much larger than that of the polystyrene repeat unit, 98.0 $cm^3$/mol. The stiffness of the polystyrene chain is thus overestimated, leading to an underestimate of the configurational entropy in the lattice model calculations. One of the limitations of rigid lattice theories for heterogeneous polymer systems is that the various species in the system may have different volumes, rendering precise specification of the reference volume impossible.

In the case of *ω*-fluorosilane polystyrene, the inconsistency in definition of the lattice volume may be resolved to a certain extent if the fluorosilane end group is considered to occupy two adjacent lattice sites, that is, if the polymer is treated as an α,*β*-functional polymer. The end group can be divided into two adjacent functional groups: group one, $CF_3(CF_2)_3-$, and group two, $-(CF_2)_2(CH_2)_2Si(CH_3)_2-$. The volume, solubility parameter, and surface tension of each of these individual end groups calculated by group contribution methods are shown in Table 3. Because the volumes of the two end groups are not identical, we set the reference volume for the α,*β*-functional polymer model to the average of the two adjacent functional groups, 126.75 $cm^3$/mol. The dashed lines in Figures 3−6 represent the theoretical ADXPS profiles when the *ω*-fluorosilane polystyrene is modeled as α,*β*-functional polymer with two adjacent functional groups at the chain end.

The optimal values of $\chi_s$ and $\chi_b$ for the α,*β*-functional polymer model were obtained by regression to the ADXPS data in similar fashion as was done for the α-functional polymer model. Figure 9 shows the total mean-squared error as a function of $\chi_s$ and $\chi_b$ calculated from regression to all of the ADXPS data for PSF5, PSF10, and PSF25. The graph shows a trough of minimum mean-squared errors that produce a large number of optimal pairs of $\chi_s$ and $\chi_b$ values. Table 4 reports a sampling of $\chi_s$ and $\chi_b$ values that fit the data along with the associated functional group surface

**Table 3. Solubility Parameter, Surface Tension, Surface Interaction Parameter, and Bulk Interaction Parameter Calculated from Group Contribution Methods for the End-Fluorosilane-Terminated Polystyrene Modeled as Either α-Functional Polymer or α,β-Functional Polymer[a]**

| | α-functional polymer | α,β-functional polymer | |
|---|---|---|---|
| reference unit | $CF_3(CF_2)_3(CF_2)_2(CH_2)_2Si(CH_3)_2-$ | $CF_3(CF_2)_3-$ | $-(CF_2)_2(CH_2)_2Si(CH_3)_2-$ |
| volume ($cm^3$/mol) | 253.5 | 105.85 | 147.6 |
| $\delta_e$ (dyn/cm) | 6.66 | 6.82 | 6.55 |
| $\gamma_e$ (dyn/cm, KS) | 20.3 | 15.9 | 16.4 |
| $\gamma_e$ (dyn/cm, HS) | 20.1 | 15.7 | 16.2 |
| $\chi_b$ | 2.54 | 0.93 | 1.62 |
| $\chi_s$(KS) | −2.68 | −1.83 | −2.24 |
| $\chi_s$ (HS) | −2.72 | −1.85 | −2.26 |

[a] Group contribution relations: KS = Koenhen and Smolder;[30] HS = Hildebrand and Scott.[29]

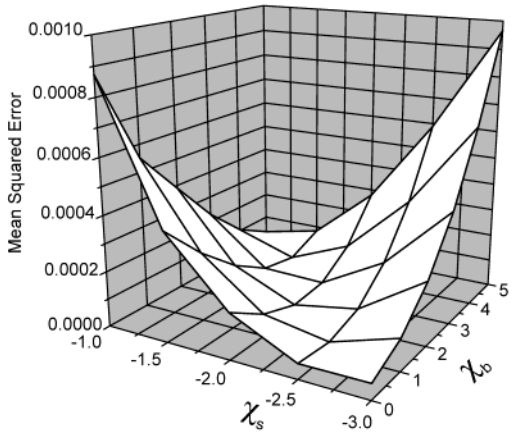


**Figure 9.** Sum of mean-squared errors between predicted and observed depth profiles for PSF5, PSF10, and PSF25 as a function of $\chi_s$ and $\chi_b$. The model predictions used to determine the mean-squared errors were based upon an α,β-functional architecture for PSF.

**Table 4. Optimal Pairs of $\chi_s$ and $\chi_b$ Values Obtained from Regression of ADXPS Data with the α,β-Functional Polymer Model and the Corresponding Total Mean-Squared Error[a]**

| $\chi_s$ | $\chi_b$ | total mean-squared error | $\gamma_e$ | $\delta_e$ |
|---|---|---|---|---|
| −1 | 5 | $3.33 \times 10^{-5}$ | 28.37 | 4.27 |
| −1.5 | 4 | $3.05 \times 10^{-5}$ | 22.55 | 5.36 |
| −2 | 2 | $3.63 \times 10^{-5}$ | 16.73 | 6.04 |
| −2.5 | 1 | $3.99 \times 10^{-5}$ | 10.91 | 6.94 |
| −3 | 0 | $5.59 \times 10^{-5}$ | 5.10 | 9.10 |

[a] The functional group surface tension and solubility parameter are calculated from eqs 2 and 3.

tension and solubility values calculated for each $\chi_s$ and $\chi_b$ pair from (2) and (3).

The optimal pairs of $\chi_s$ and $\chi_b$ values were again determined by the intersection of the experimental parameter sets with the relationship between the two parameters determined by group contribution as shown in Figure 10. The optimal values obtained from the Hildebrand and Scott group contribution method are $\chi_s = -2.18$ and $\chi_b = 1.59$. Those obtained from the Koenhen and Smolder group contribution method are $\chi_s = -2.15$ and $\chi_b = 1.62$. To determine whether these values are physically reasonable and self-consistent, we compare them to values calculated from (2) and (3) using the group contribution estimates of $\gamma_e$ and $\delta_e$ presented in Table 4. Group contribution calculations yield $\chi_s = -1.83$ and $\chi_b = 0.93$ for the first adjacent end group and $\chi_s = -2.24$ and $\chi_b = 1.62$ for the second adjacent end group. Since an "average" functional group volume was employed in the lattice calculations, it is appropriate

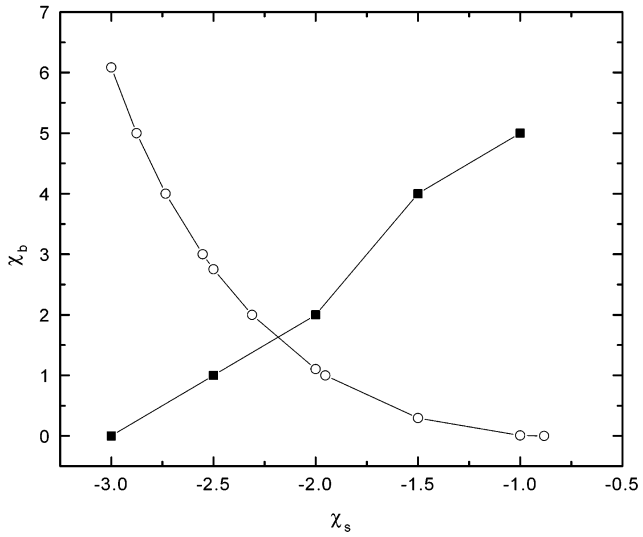


**Figure 10.** Relationship between $\chi_s$ and $\chi_b$: predicted by the Hildebrand and Scott formulas (circles) and obtained from optimal comparisons to the data when PSF is modeled as an α,β-functional polymer (squares).

to average the interaction parameters. The average of group contribution calculations yields $\chi_s = -2.04$ and $\chi_b = 1.28$, comparing quite favorably with the results $\chi_s = -2.18$ and $\chi_b = 1.59$ obtained from regression of experimental ADXPS data with the α,β-functional polymer model. We therefore conclude that experimental ADXPS data for *ω*-fluorosilane polystyrene is well represented by the lattice model as long as the reference volume is appropriately selected.

ADXPS data for PSF5 is compared to that for a 60% blend of PSF5.4 with PS4 in Figure 11. The concentration depth profiles are similar for both the "neat" and blend system, demonstrating the strong tendency for surface segregation of *ω*-fluorosilane polystyrene. The solid and dotted lines represent the predictions from the α-functional polymer model using the optimal values of $\chi_s = -3.34$ and $\chi_b = 4.7$. The dashed and dashed−dotted lines represent the α,β-functional polymer model predictions assuming an architecture with two adjacent functional groups at the chain end using the optimal values of $\chi_s = -2.18$ and $\chi_b = 1.59$. The same optimal parameter values obtained by regression of the previous "neat" systems (i.e., PSF5, PSF10, and PSF25) therefore also give good representation of ADXPS data for the blends of PSF5.4 with PS4.

The fluorine-to-carbon ratios for various compositions of PSF5.4 blended with PS4 are shown in Figure 12 for four different takeoff angles. For all takeoff angles the fluorine-to-carbon ratio increases with increasing concentration of the *ω*-fluorosilane polystyrene in the blend.

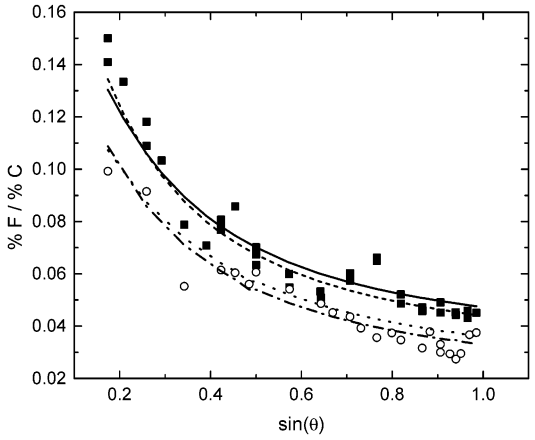


**Figure 11.** Comparison of angle resolved data for 100% PSF5 (squares) and a 60% blend of PSF5.4 with PS4 (circles). The solid line is the model prediction for 100% PSF5 assuming it is a blend of 89% α-functional polymer ($r_\alpha = 19$, $\chi_s = -3.34$, $\chi_b = 4.7$) with 11% nonfunctional polymer ($r_n = 18$). The dashed line is the model prediction for 100% PSF5 assuming it is a blend of 89% α,β-functional polymer ($r_{\alpha,\beta} = 39$, $\chi_s = -2.18$, $\chi_b = 1.59$) with 11% nonfunctional polymer ($r_n = 38$). The dotted line is the model prediction for the 60% blend of PSF5.4 with PS4 assuming that it is a ternary blend of 40.2% α-functional polymer ($r_\alpha = 20$, $\chi_s = -3.34$, $\chi_b = 4.7$), 19.8% nonfunctional polymer ($r_n = 19$), and 40% nonfunctional polymer ($r_n = 15$). The dashed−dotted line is the model prediction for the 60% blend of PSF5.4 with PS4 assuming that it is a ternary blend of 40.2% α,β-functional polymer ($r_{\alpha,\beta} = 40$, $\chi_s = -2.18$, $\chi_b = 1.59$), 19.8% nonfunctional polymer ($r_n = 39$), and 40% nonfunctional polymer ($r_n = 28$).

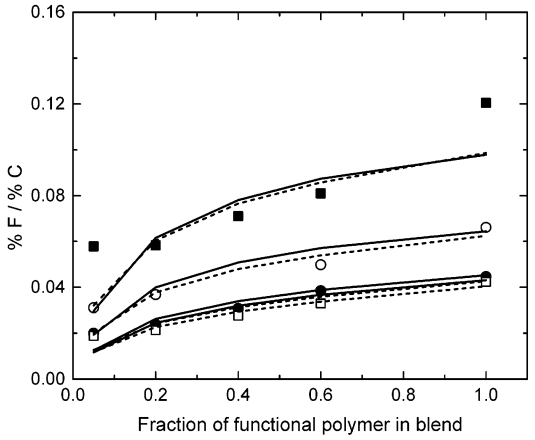


**Figure 12.** Fluorine-to-carbon atomic ratios for blends of PSF5.4 with PS4 as a function of blend composition. The takeoff angles were 15° (filled squares), 30° (open circles), 62° (filled circles), and 75° (open squares). The solid lines are predictions for blends of α-functional polymer (treated as a binary mixture containing 67% α-functional polymer with $r_\alpha = 20$, $\chi_s = -3.34$, $\chi_B = 4.7$ and 33% nonfunctional polymer with $r_n = 19$) with nonfunctional polymer ($r_n = 15$). The dashed lines are predictions for blends of α,β-functional polymer (treated as a binary mixture containing 67% α,β-functional polymer with $r_{\alpha,\beta} = 40$, $\chi_s = -2.18$, $\chi_b = 1.59$ and 33% nonfunctional polymer with $r_n = 38$) with nonfunctional polymer ($r_n = 28$).

The highest ratio of fluorine to carbon occurs at the lowest takeoff angle, 15°, corresponding to the shallowest depth probed by the experiment. The lattice calculations assuming α-functional and α,β-functional architectures, solid and dashed lines, respectively, again provide excellent representations of the data when optimal $\chi_s$ and $\chi_b$ values are employed.

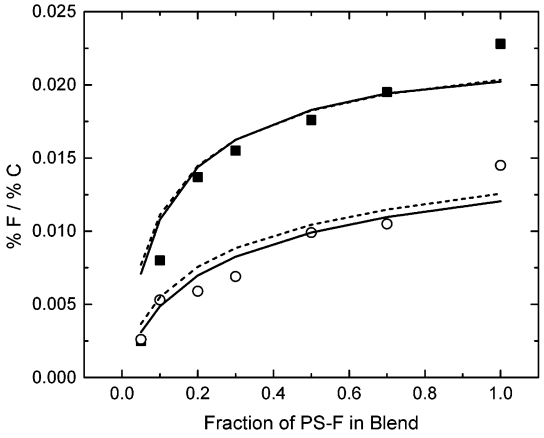


**Figure 13.** Fluorine-to-carbon atomic ratios for blends of PSF17 (squares) or PSF35 (circles) with PS35. The solid lines are predictions assuming PSF is an α-functional polymer with $\chi_s = -3.34$ and $\chi_b = 4.7$. The dashed lines are predictions assuming PSF is an α,β-functional polymer with $\chi_s = -2.18$ and $\chi_b = 1.59$.

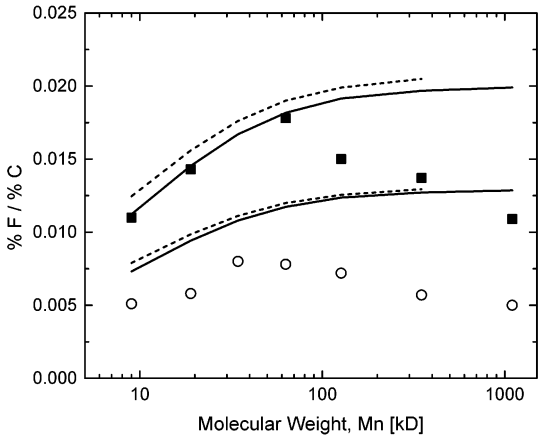


**Figure 14.** Fluorine-to-carbon atomic ratios for blends containing 10% PSF17 and 90% polystyrene of varying molecular weight. The takeoff angles are 62° (circles) and 30° (squares). The solid lines are model predictions assuming PSF is an α-functional polymer with $\chi_s = -3.34$ and $\chi_b = 4.7$. The dashed lines are model predictions assuming PSF is an α,β-functional polymer with $\chi_s = -2.18$ and $\chi_b = 1.59$.

Figure 13 shows the effects of molecular weight and composition on the fluorine-to-carbon atomic concentration ratios. Surface segregation of the fluorosilane end groups increases with concentration of the end-fluorinated polymer. Segregation appears to be stronger for the lower molecular weight ω-fluorosilane polystyrene, but this effect is related to the fact that the overall fluorine content of the blend is higher for lower molecular weight polymer. The lattice theory (solid and dashed lines), employing optimal interaction parameters, again provides an excellent representation of the data.

A more in-depth investigation of molecular weight effects is shown in Figure 14. The figure shows how the ratio of fluorine-to-carbon atomic concentration depends on molecular weight of the nonfunctional polystyrene in blends containing 10% PSF17. As the molecular weight of the matrix increases, there is an initial increase in the ratio of fluorine to carbon increases for both takeoff angles. The ratio of fluorine to carbon decreases, however, for molecular weights greater than 127 kDa. The latter trend for high molecular weights is contrary to both the results of the simulations and to

what would be expected from simple consideration of free energy terms. The theoretical profiles (solid and dashed lines) show good agreement with experiment at low molecular weights but continue to increase as the matrix molecular weight increases. The expected continual increase in surface segregation is associated with the reduction of mixing entropy when the matrix molecular weight is increased. Since the total concentration of end groups and the end group surface tension are fixed in this series of experiments, the degree of surface segregation is a function only of the free energy required for demixing surface-adsorbed functional polymer from the bulk. Because the end group composition is fixed, the enthalpic contributions are independent of the matrix molecular weight, and changes in the degree of surface segregation are due exclusively to changes in the entropy of mixing. The reduction in mixing entropy upon increase in matrix molecular weight decreases the free energy of demixing and thus should lead to increased surface segregation of end-functional polymer when the molecular weight of the nonfunctional polymer is increased.

During review of this article, it was suggested that the discrepancy between experiment and theory observed at high molecular weights may be associated with the onset of macroscopic phase separation between end-functional and nonfunctional polymers above some critical molecular weight of the polystyrene matrix. In previous work,[31] we have shown that the phase behavior for blends of end-functional polymers (polymer 1) with nonfunctional polymers (polymer 2) is well represented by Flory−Huggins theory, when the interactions are modeled using binary interaction theory. If we treat PSF17 as a random copolymer with a volume fraction, $x$, of end groups, the effective interaction parameter for blends of nonfunctional polystyrene with PSF17 can be defined as[32]

$$\chi_{\text{effective}} = \chi_{\text{er}}(1 - x)^2 \tag{12}$$

The subscripts r and e refer to the repeat unit of polymer and the end group, respectively. The volume fraction of end groups in PSF17 is $x = 0.016$, and the optimal bulk interaction parameter between polystyrene and the fluorosilane end group, obtained from regression of the ADXPS data, is $\chi_b = \chi_{er} = 1.59$. The effective interaction parameter for the blends with 10% PSF17, calculated from (12), is therefore $\chi_{\text{effective}} = 0.0004$. For this effective interaction parameter, Flory−Huggins theory predicts that blends of nonfunctional polystyrene with 10% PSF17 are miscible for all molecular weights of nonfunctional polystyrene. The discrepancy between theory and experiment therefore does not appear to be associated with the onset of macroscopic phase separation.

We do not have an obvious explanation why the lattice model would be applicable at low matrix molecular weights but fail at high molecular weights. We suspect, however, that the discrepancy between experimental results and theoretical predictions found at high molecular weight may be associated with the fact that equilibrium is difficult to attain for such high molecular weights. The annealing times of 2 h for the PS127 blend and 20 h for the PS350 and PS1100 blends may not have been sufficient for PSF17 to segregate to the surface and reach its equilibrium concentration.


## Summary

Angle-dependent X-ray photoelectron spectroscopy (ADXPS) is applied to measure fluorosilane end group concentration depth profiles for blends of *ω*-fluorosilane polystyrene with nonfunctional polystyrene. The *ω*-fluorosilane polystyrenes segregate preferentially to the surface as a result of the low surface energy fluorosilane end groups. The degree of end group surface segregation is found to increase with concentration of end-functional polymer and to decrease with molecular weight of the end-functional polymer. An increase in molecular weight of the nonfunctional polystyrene causes an increase in end group segregation up to a molecular weight of 127 kDa and then a decrease for higher molecular weights. A self-consistent mean-field lattice theory is developed to model the properties of blends of surface-active end-functional polymers and nonfunctional polymers. The lattice theory provides an excellent representation of experimental ADXPS data over a wide range of blend compositions and blend constituent molecular weights when the *ω*-fluorosilane polystyrene is modeled as an α,*β*-terminated polymer where the fluorosilane end group is assumed to occupy two lattice sites. Regression of the lattice model to the data provides optimal estimates of $\chi_s = -2.18$ and $\chi_b = 1.59$ respectively for the surface and bulk interaction parameters—values that compare favorably with estimates obtained from group contribution calculations.


**Acknowledgment.** This material is based on work supported by, or in part by, the US Army Research Office and Grant DAAD19-00-1-0104 and the Polymers Program of the National Science Foundation under Grants DMR-98-09687 and DMR-02-14363.

## Appendix

The total solubility parameter, $\delta$, is often described in terms of different contributions due to dispersive ($\delta_{\text{disp}}$), polar ($\delta_{\text{polar}}$), and hydrogen-bonding ($\delta_{\text{h-bond}}$) interactions:[33]

$$\delta^2 = (\delta_{\text{disp}})^2 + (\delta_{\text{polar}})^2 + (\delta_{\text{h-bond}})^2 \tag{A1}$$

Applying group contributions methods it follows that the three solubility parameters can be calculated from[33]

$$\delta_{\text{disp}} + \sum F_{i,\text{disp}}/\nu_m \tag{A2}$$

$$\delta_{\text{polar}} + \sum F_{i,\text{polar}}/\nu_m \tag{A3}$$

$$\delta_{\text{h-bond}} + \sum F_{i,\text{h-bond}}/\nu_m \tag{A4}$$

where $\nu_m$ is the molar volume of the segment under consideration. Each segment is considered to comprise a number of subunit fragments, $i$, with molar attraction constants $F_{i,\text{disp}}$, $F_{i,\text{polar}}$, and $F_{i,\text{h-bond}}$ for dispersion, dipole, and hydrogen bond forces, respectively, and the solubility parameters are calculated by summing over the contributions of each subunit.

The hydrogen bond and dipole forces can be neglected for *ω*-fluorosilane polystyrene because interactions should be only of a dispersive nature. Once the end group solubility parameter is calculated, the end group surface tension is obtained by applying group contribution relationships proposed by Hildebrand and Scott[29]

$$\gamma_e = 0.07147(\delta_{disp})^2(\nu_e)^{1/3} \quad \text{(A5)}$$

or Koenhen and Smolders[30]

$$\gamma_e = (\delta_{disp}{}^2 + \delta_{polar}{}^2)(\nu_e)^{1/3}/13.8 \quad \text{(A6)}$$

## References and Notes


(1) Wu, S. *Polymer Interfaces and Adhesion*, 1st ed.; Marcel Dekker: New York, 1982.
(2) Pan, D. H.; Prest, W. M. J. *J. Appl. Phys.* **1985**, *58*, 2861.
(3) Schmitt, R.; Gardella, J. A., Jr.; Magill, J. H.; Salvati, L., Jr. *Macromolecules* **1985**, *18*, 2675.
(4) Bhatia, Q. S.; Pan, D. H.; Koberstein, J. T. *Macromolecules* **1988**, *21*, 2166.
(5) Gaines, G. L., Jr. *J. Chem. Phys.* **1969**, *73*, 3143.
(6) Elman, J. F.; Johs, B. D.; Long, T. E.; Koberstein, J. T. *Macromolecules* **1994**, *27*, 5341.
(7) Koberstein, J. T. Tailoring Polymer Interfacial Properties by End Group Modification. In *Polymer Surface, Interfaces and Thin Films*; Series on Directions in Condensed Matter Physics; World Scientific Publishing: Singapore, 2000; pp 115−181.
(8) Koberstein, J. T. Polymer Surface Properties. In *Encyclopedia of Polymer Science and Technology*; John Wiley & Sons: New York, 2001.
(9) Hunt, M. O. J.; Belu, A. M.; Linton, R. W.; DeSimone, J. M. *Macromolecules* **1993**, *26*, 4854.
(10) Affrossman, S.; Hartshorne, M.; Kiff, T.; Pethrick, R. A.; Richards, R. W. *Macromolecules* **1994**, *27*, 1588.
(11) Hopkinson, I.; Kiff, F. T.; Richards, R. W.; Bucknall, D. G.; Clough, A. S. *Polymer* **1997**, *38*, 87.
(12) Schaub, T. F.; Kellogg, G. J.; Mayes, A. M.; Kulasekere, R.; Anker, J. F.; Kaiser, H. *Macromolecules* **1996**, *29*, 3982.
(13) Mason, R.; Jalbert, C. J.; O'Rourke-Muisener, P. A.; Koberstein, J. T. *Adv. Colloid Interface Sci.* **2001**, *94*, 1.
(14) Yuan, C.; Ouyang, M.; Koberstein, J. T. *Macromolecules* **1999**, *32*, 2329.
(15) Scheutjens, J. M. M. H.; Fleer, G. J. *J. Phys. Chem.* **1979**, *83*, 1619.
(16) Theodorou, D. N. *Macromolecules* **1988**, *21*, 1422.
(17) Theodorou, D. N. *Macromolecules* **1988**, *21*, 1411.
(18) Jalbert, C. J.; Koberstein, J. T.; Hariharan, A.; Kumar, S. K. *Macromolecules* **1997**, *30*, 4481.
(19) O'Rourke-Muisener, P. A.; Kumar, S. K.; Koberstein, J. T. *Macromolecules* **2003**, *36*, 771.
(20) Jalbert, C. J.; Balaji, R.; Bhatia, Q. S.; Salvati, L., Jr.; Yilgor, I.; Koberstein, J. T. *Macromolecules* **1994**, *27*, 2409.
(21) Jalbert, C. J. Ph.D. Dissertation, University of Connecticut, 1993.
(22) Hariharan, A. H.; Kumar, S. K.; Russell, T. P. *Macromolecules* **1990**, *23*, 3584.
(23) Hariharan, A. H.; Kumar, S. K.; Russell, T. P. *Macromolecules* **1991**, *24*, 4909.
(24) Shull, K. As applied in ref 11.
(25) Van Krevelyn, D. W. *Properties of Polymers: Their Estimation and Correlation with Chemical Structure;* Elsevier: Amsterdam, 1976.
(26) Fadley, C. S. *Prog. Solid State Chem.* **1976**, *11*, 265.
(27) Ashley, J. C. *IEEE Trans. Nucl. Sci.* **1980**, *NS-27*, 1454.
(28) Brandup, J.; Immergut, E. H. *Polymer Handbook*, 3rd ed.; John Wiley and Sons: New York, 1989.
(29) Hildebrand, J. H.; Scott, R. L. *Solubility of Nonelectrolytes*; D. Van Nostrand: Princeton, NJ, 1950.
(30) Koenhen, D. M.; Smolder, C. A. *J. Appl. Polym. Sci.* **1975**, *19*, 1163.
(31) Lee, M. H.; Fleischer, C. A.; Morales, A. R.; Koberstein, J. T.; Koningsveld, R. *Polymer* **2001**, *42*, 9163.
(32) Lipatov, Y. S.; Nesterov, A. E. *Thermodynamics of Polymer Blends*; Technomic: Lancaster, 1997.
(33) Hansen, C. M. *J. Paint Technol.* **1967**, *39*, 104.


MA021623V